



## Research Article

## Effect of Corner Radii on the Thermal & Fluid Flow Performance of the Laminar Flow through Rectangular Micro Channel

S.Subramanian<sup>A</sup>, K.S.Sridhar<sup>B</sup> and C.K.Umesh<sup>C</sup>

<sup>A</sup>Microwavetube Research & Development Center, Jalahalli, Bangalore, India

<sup>B</sup>PES Institute of Technology, 100 feet Ring Road, BSK III Stage, Bangalore, India

<sup>C</sup>University Visvesvaraya College of Engineering, KR Circle, Bangalore, India

Accepted 25 Dec 2014, Available online 31 Dec 2014, Vol.4, No.4 (Dec 2014)

### Abstract

*Metallic micro channels have the advantage of high thermal conductivity to strength ratio. The recent advances in the manufacturing processes, has increased the feasibility of realizing metallic micro channels with close dimensional control. Presently, various types of micro manufacturing processes are available for the realization of the metallic micro channels. However it is not practical to manufacture any dimensional feature with sharp corner. Depending on the choice of the manufacturing process, the corners get rounded to varying degree. When compared with the dimensions of micro channels the magnitude of the corner radius is considerable. In this paper an attempt has been made to study numerically the effect of corner radius on the performance of the micro channels. Commercially available computational fluid dynamics software ANSYS CFX was used for the simulation of micro channels performance. The thermal & fluid flow performance of the micro channel was simulated by varying the corner radius from 50 microns to 200 microns. The coolant flow velocities were varied from 0.48m/s to 1.27m/s. The Temperature dependent material properties have been used in the analysis. The simulation results were validated using published literature.*

**Keywords:** Corner radius on micro channels, Copper micro channel, laminar flow in micro channels, Thermal & fluid flow performance of micro channels, Manufacture of micro channels

### 1. Introduction

Micro channels are attractive due its evident advantage & usefulness (D.B.Tuckerman & R.F.W.Pease, 1981). A thermal resistance of 0.09°C/W over one cm<sup>2</sup> area was achieved for a heat load of 790W/cm<sup>2</sup>. The substrate temperature rise was 71°C above water inlet temperature. From then on silicon micro channels have been under active consideration (K.Kawano *et al.*, 2001; M.J. Khol *et al.*, 2005; and R.Chein *et al.*, 2007). However metallic micro channels have been a potential attraction for electronics cooling applications. The metallic micro channels were manufactured on copper & aluminium by mold replication techniques (Fanghua Mei *et al.*, 2008) using engineered metallic mold inserts. The main focus of the study was on the friction factor & transients effects. The merits and limitations of various manufacturing processes such as LIGA, chemical etching, stereo lithography, micromachining & diffusion bonding that are suitable for micro channel fabrication have been reported (Sean Asman *et al.*, 2006). B.A.Jasperson *et al.*, 2010 described about the recent advances in micromachining technologies which enable us to machine very fine features demanded by metallic micro channel heatsinks with better tolerance control. The nickel-based micro-channel cooling

plate with 128 numbers of micro channels having the hydraulic diameter of 70 micrometer were fabricated on a glass substrate using a two-layer electroforming process (A. J. Pang, M.P.Y. Desmulliez *et al.*, 2004). Nitrogen gas was used as the coolant fluid for the micro channel plate. The hydraulic performance has been tested & analyzed. A comprehensive overview of works on micro channel research reported about the (C.B.Sobhan and S.Garimella 2001) little agreement between the results of different researchers. The discrepancy in the results were attributed to surface roughness, non uniformity of channel geometry, boundary conditions, errors in the instrumentation, entrance & exit effects. The pressure drop & heat transfer characteristics of oxygen free copper based micro channels for the Reynolds numbers from 139 to 1672 have been reported (Weilin Qu & I. Mudawar, 2002). It was concluded that the Navier-Stokes equations are adequate enough to predict the performance of micro channels. A novel integral micro-channel heat sink directly on the back-metallization layer of copper bonded with ceramic substrate of the semiconductor junction was fabricated and tested (L.D Stevanovic *et al.*, 2010). It was reported that the micromilled micro channels performed better than laser ablated samples.

Micromachining is one of the promising cutting processes which can be reliably used for the manufacture of micro channels. Hence micro-milling was employed for

\*Corresponding author: S.Subramanian

the manufacture of micro channel on copper. In this paper Rectangular micro channel having 500micron width and 1500 micron depth with hydraulic diameter of 0.75mm is used as the bench mark problem. The thermal & fluid flow performance of the above copper based micro channel heatsink was simulated using the commercial Computational fluid dynamics code ANSYS CFX. The results of the numerical simulation have been validated with the published literature data. The effect of micro channel corner radius on the fluid flow & thermal performance has been studied by varying the corner radius from 50microns to 200 microns.

## 2. CFD simulation

Conjugate heat transfer simulation was performed by varying the inlet fluid velocity, heat load & the corner radius. Since there is symmetry along the flow axis, only half the size of a micro channel has been modeled in three dimensional coordinate to minimize the computational load. The model consists of inlet, micro channel region and outlet. The meshed half channel model is shown in Fig: 1

## 3. Mesh independency check

Mesh dependency check was carried out by increasing the mesh elements of the model for the same set of boundary conditions. The minimum number of elements to achieve the consistent results between consecutive analyses was found to be 871663 as shown in Fig 2. The fluid boundaries were inflated by 8 layers for 50 micrometer thickness. The convergence criteria for residues were set to  $10^{-6}$  while activating high resolution scheme.

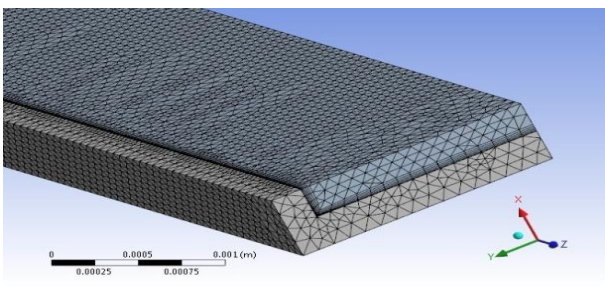


Fig 1: Meshed model of half channel

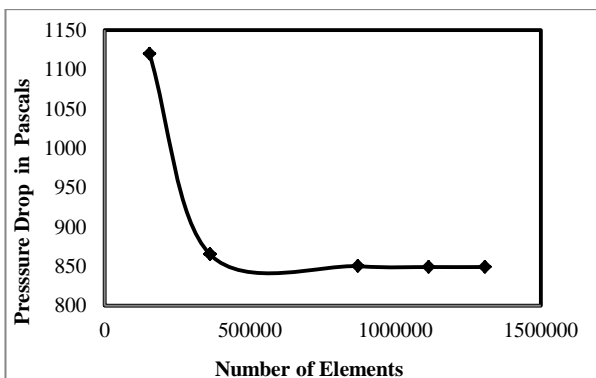


Fig 2: Effect of number of elements on simulation

## 4. Boundary conditions used

Mass flow rate was specified at the inlet while pressure boundary condition was applied at the outlet. Symmetric boundary condition was assigned to the sides. Uniform heat flux was applied to the heatsink surface at the bottom. Two different levels of heat loads such as  $65 \text{ W/cm}^2$  and  $32 \text{ W/cm}^2$  were used for the simulation. The top of the micro channel heat sink was considered to be bonded with adiabatic cover. The velocity was varied from 0.48m/s to 1.27 m/s. The Reynolds number of the fluid flow at the inlet, ranged from 503 to 1197.

## 5. Material properties

It is important to use temperature dependent properties of coolant as it influences the simulation results to larger extent (S.Subramanian et al, 2014). The temperature dependence of the properties of water was modeled using CEL commands in ANSYS CFX pre. Whereas the constant thermal conductivity of  $K_{cu} = 387.6 \text{ W/mK}$  was used for the heat sink. The density, specific heat, thermal conductivity and dynamic viscosity of the coolant fluid have been calculated at the mean fluid temperature using temperature dependent material properties formulae.

## 6. Analytical model

The flow is found to be always in the thermally developing region for the 25mm long micro channel heat sink. The assumption of fully developed flow is not suitable. Hence the analytical model (L Biswal et al, 2009) consisting of components for developing & developed flow has been used for comparison. The analytical calculations were performed using the formulae listed from (1) to (6).

Thermal resistances:

$$R_{total} = \frac{T_{max} - T_{in}}{Q} = R_{conduction} + R_{fluid} + R_{fin} \quad (1)$$

$$R_{conduction} = \frac{1}{K_{hs} + A_{hs}}$$

$$R_{fluid} = \frac{1}{Cp_f \mu_f} \frac{1}{Re} \frac{1 + \beta}{1 + \alpha} \frac{L_{hs}}{A_{hs}}$$

$$R_{fin} = \frac{1}{Nu} \frac{1}{K_f} \frac{1 + \beta}{1 + 2\alpha} \frac{2\alpha}{1 + \alpha\eta} \frac{W_{ch}}{A_{hs}}$$

Fin Efficiency and Reynolds number:

$$\eta = \frac{\tanh(m\alpha)}{m\alpha} R_e = \frac{\rho_f u_m D_h}{\mu_f} \quad m = \sqrt{Nu} \frac{1 + \alpha}{\alpha \beta} \frac{K_f}{K_{hs}} \quad (2)$$

Hydraulic Diameter and aspect ratios:

$$D_h = \frac{(2W_{ch}L_{ch})}{(W_{ch} + L_{ch})} \quad \alpha = \frac{L_{ch}}{W_{ch}} \quad \beta = \frac{W_{fin}}{W_{ch}}$$

Mean fluid velocity in the channel:

$$u_m = \frac{v_f}{(NW_{ch}L_{ch})} \quad N = \frac{(W_{hs} + W_{fin})}{(W_{ch} + W_{fin})} \quad (3)$$

Poiseuille numbers:

$$f \cdot Re = [\{3.2 (Re D_h / L_{hs})^{0.57}\}^2 + (4.7 + 19.64 G)^2]^{\frac{1}{2}}$$

$$G = (\alpha^{-2} + 1) / (\alpha^{-1} + 1)^2 \quad \sigma = \frac{NW_{ch}}{W_{ch}}$$

$$K = 0.6 \sigma^2 - 2.4 \sigma + 1.8 \tag{4}$$

Pressure drop across the channel:

$$\Delta P = \frac{\rho_f u_m^2}{2} (4f \frac{L_{hs}}{D_h} + K) \tag{5}$$

Nusselts number for developing & developed flow:

$$Nu_u = [\{2.22(Re P_r D_h / L_{hs})\}^{0.33} + (8.31G - 0.02)]^{\frac{1}{3}}$$

$$Nu_u = (h D_h) / K_f \tag{6}$$

**7. Validation**

The CFD simulation results were validated using published data o (Y.J Lee et al, 2013) & analytical estimates (L.Biswal et al, 2009). The influence of the Reynolds number of the inlet flow over the pressure drop is plotted in figure 7. The pressure drop increased with respect to inlet flow Reynolds number. The simulated results were found to closely match with Published data & analytical results which are shown in Fig 3. The simulated results and analytical estimate were found to be close by 2.2% to the published data.

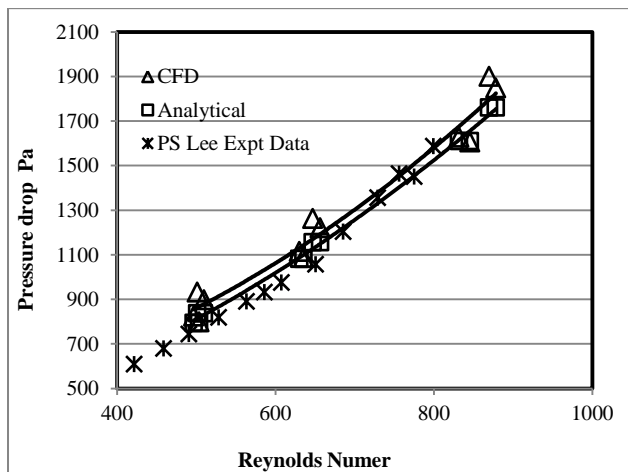


**Fig 3:** Variation of Pressure drop with Reynolds number

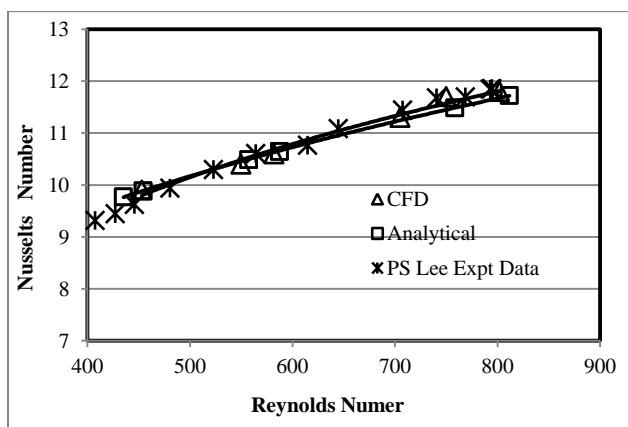


**Fig 4:** Variation of Nusselts number with Reynolds number

The influence of the Reynolds number of the inlet fluid velocity over the Nusselts number is shown below figure 8. The nusselts number increased as the Reynolds number increased. Analytical & CFD simulation results were closely matching with the experimental and published data. Hence the CFD simulation has been taken as the benchmark for the further comparison studies. However for every input variation the grid dependency study was carried out to ensure dependable results

**8. Effect of Corner Radius on the performance**

The manufacturing process such as Micromilling, Electro discharge machining, Electrochemical etching, Slitting, Broaching, Sawing, Extrusion etc., are reported to be suitable for machining micro channel on the metals( S. Ashman et al, 2006). Micromilling of rectangular micro channel requires miniature sized cutting tools. The Micromilling machine is required to have a higher spindle speed of around 6000RPM to 8000 RPM due to the smaller size of the milling tool. Nearly rectangular channels can be milled using milling machine. The milling tool exerts considerable cutting force to induce plastic deformation while cutting the metal. The micro channel walls must be thick enough to withstand the cutting force which limits the feature size of the walls. Hence channels with fine dimensions are dictated by cutting tool force. If the rectangular channels were cut using WEDM process or tools with rounded cutting edges, there will be corner radius in the channel along the cutting axis as shown in Fig 5. These corner radii affect the hydraulic diameter of the micro channels. Hence the effect of corner radius was simulated to estimate the extent of influence of corner radius on the performance of the micro channel.



**Fig 5:** Rectangular micro channel with corner radius

The Pressure contours of the rectangular micro channel with sharp corner and that of the channel having 100micrometer corner radius is shown in Fig 6 and Fig 7.

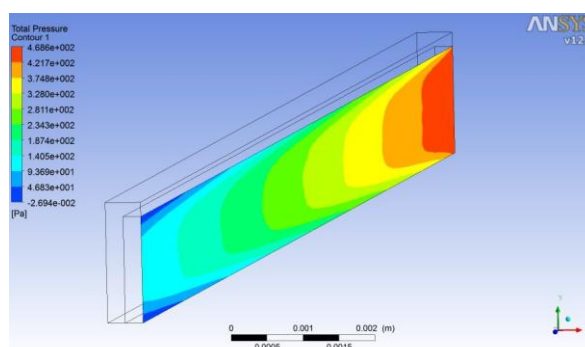


**Fig 6:** Pressure contour for rectangular channel

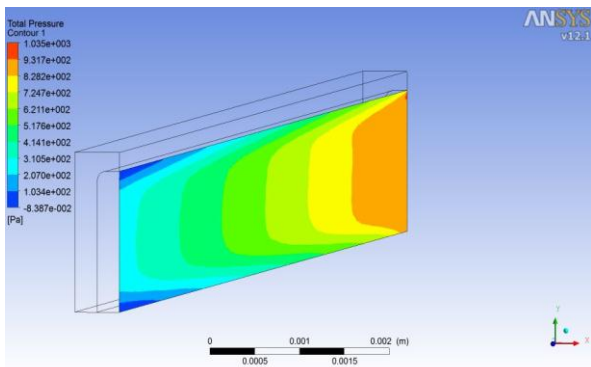


Fig 7: Pressure contour for 100microns corner radius

The pressure contour is varying along the flow. The pressure is reducing towards the exit. The magnitude of pressure drop is nearly the same irrespective of corner radius values. The velocity contour of the flow is shown in the Fig 8 and Fig 9. The velocity variation indicates it is a fully developed flow. The velocity is found to vary near the walls and is found to reach maximum at the center.

The CFD simulations were carried out for two different heat loads namely 32 W/cm<sup>2</sup> and 65 W/cm<sup>2</sup>. The effect of inlet velocities on the pressure drop with respect to different corner radii for 32W/cm<sup>2</sup> is shown in figure 10. The effect of inlet velocities on the pressure drop with respect to different corner radii for 65W/cm<sup>2</sup> heat load is shown in figure 11. The pressure drop increases with inlet velocity as expected. The variation in the pressure drop is found to be within 3% for both the cases

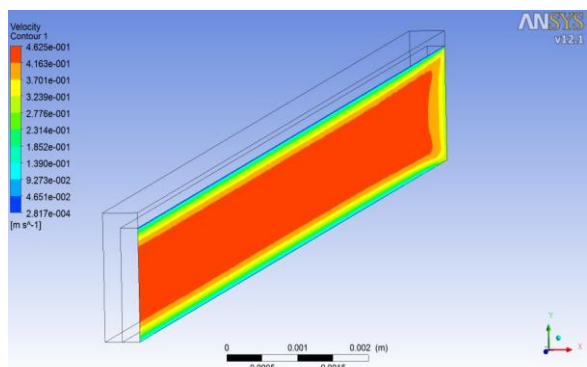


Fig 8: Velocity Contour for rectangular channel

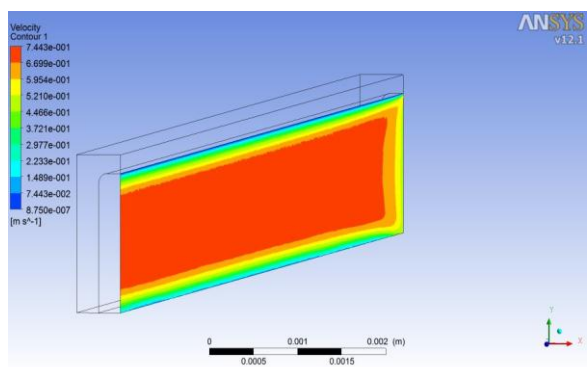


Fig 9: Velocity Contour for 100microns corner radius

The effect of inlet velocities on the heat transfer coefficient with respect to different corner radii for 32 W/cm<sup>2</sup> heat load is shown in figure 12. The effect of inlet velocities on the heat transfer coefficient with respect to different corner radii for 65 W/cm<sup>2</sup> heat load is shown in figure 13. Heat transfer coefficient is found to vary maximum by 3.5% for corner radius having 100 microns for both heat loads. The variation is found to be below 2.5% for the corner radius other than 100 microns. The heat transfer coefficient is increasing with heat loads for all the values of the corner radii.

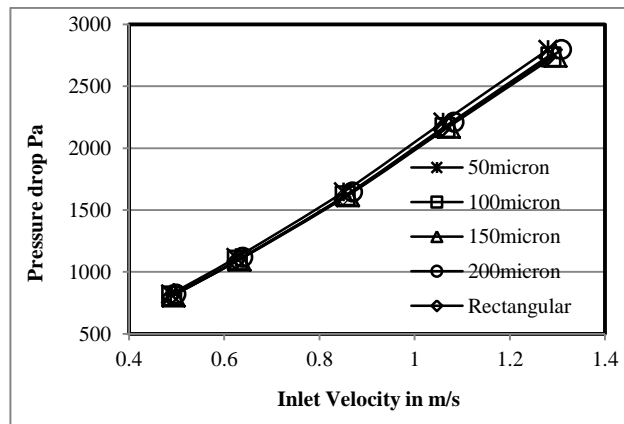


Fig 10: Velocity Vs pressure drop for 32W/cm<sup>2</sup>

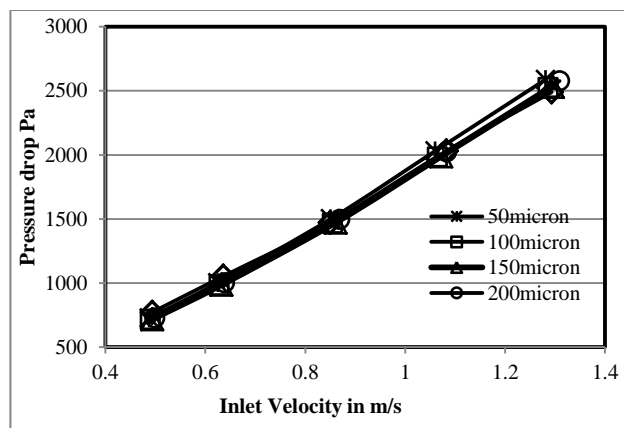


Fig 11: Velocity Vs Pressure drop for 65W/cm<sup>2</sup>

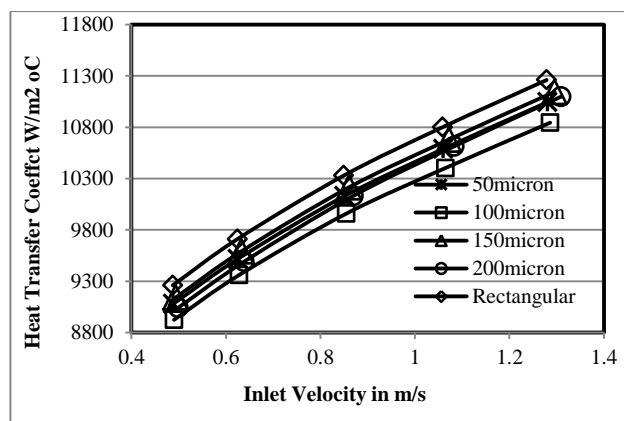
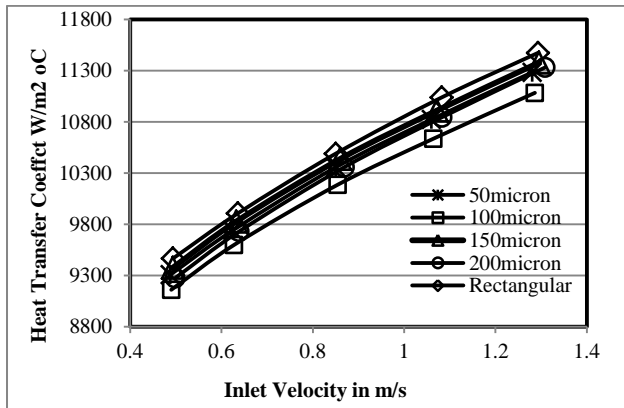
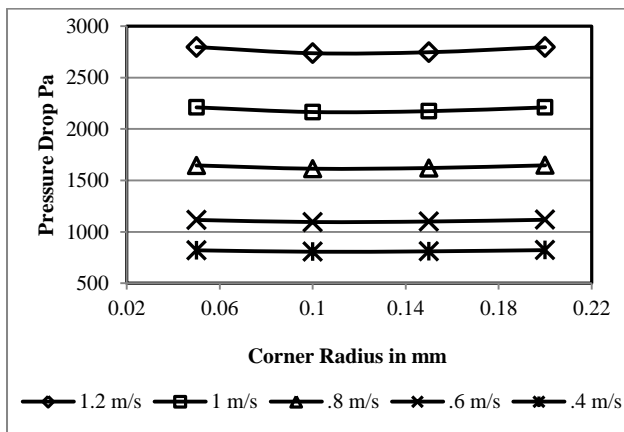


Fig 12: Velocity Vs Heat transfer coefficient for 32W/cm<sup>2</sup>



**Fig 13:** Velocity Vs Heat transfer coefficient for 65W/cm<sup>2</sup>

The effect of corner radius over pressure drop with respect to different inlet velocities for 32W/cm<sup>2</sup> heat load is shown in figure 14.



**Fig 14:** Corner radius Vs Pressure drop for 32W/cm<sup>2</sup>

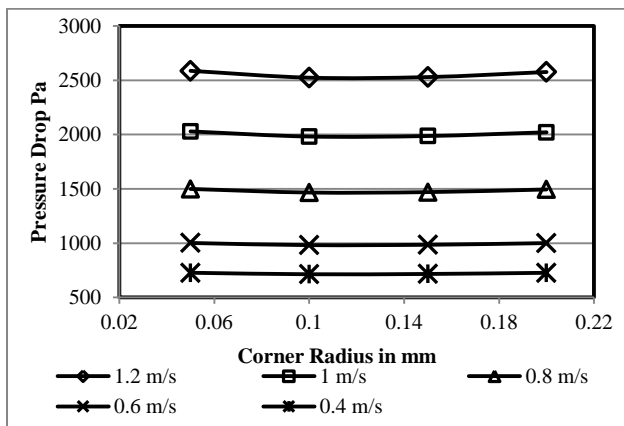


**Fig 15:** Corner radius Vs Pressure drop for 65W/cm<sup>2</sup>

The effect of corner radius over pressure drop with respect to different inlet velocities for 65W/cm<sup>2</sup> heat load is shown in figure 15. Higher the velocity higher is the pressure drop. As the heat load is increased the maximum pressure drop for the given velocity is found to be lesser. This is due to the reason that the pressure drop depends on the mean fluid temperature. The mean fluid temperature increases with the heat loads. The fluid viscosity reduces

as the mean fluid temperature increases leading to the reduction of pressure drop. However the variation of pressure drop due to the variation of corner radii is marginal in all the cases.

**Conclusions**

Thermal & fluid flow performance of Plate fin micro channel having 500 micrometers width and 1500 micrometers depth was simulated using ANSYS CFX incorporating temperature dependent material properties. The CFD simulated results were validated using published data and analytical calculations. The results of analytical calculation matched closely with simulation results & published data. The variation of the pressure drop with respect to corner radii was found to be below 3%. The heat transfer coefficient was found to vary a maximum of 3.5% for 100micrometer radius. When the heat load is increased the pressure drop is found to reduce. Whereas the heat transfer coefficient is found to increase with heat load. Since the corner radius affects the hydraulic diameter, the above variations in the pressure drop & heat transfer coefficient is attributed to influence of corner radius on the hydraulic diameter.

**Nomenclature**

- $R_e$  - Reynolds number
- $R_{total}$  - Total thermal resistance
- $R_{conduction}$  - Conductive thermal resistance
- $R_{fluid}$  - Fluid Capacitive thermal resistance
- $R_{fin}$  - Fin thermal resistance
- $A_{hs}$  - Area of heat sink
- $L_{hs}$  - Length of heat sink
- $K_{hs}$  - Thermal conductivity of heatsink
- $Q$  - Total heat load
- $T_{max}$  - Maximum heat sink temperature
- $T_{in}$  - Fluid inlet temperature
- $C_{pf}$  - Specific heat of fluid
- $\mu_f$  - Viscosity of fluid
- $f$  - friction factor
- $L_{ch}$  - Length of micro channel
- $W_{ch}$  - Width of microchannel
- $\alpha$  - Aspect ratio of microchannel
- $\beta$  - Ratio of fin width to channel width
- $\eta$  - Fin efficiency
- $G$  - Geometric parameter
- $K$  - Pressure loss coefficient
- $\rho_f$  - Fluid density
- $U_m$  - Average flow velocity
- $\Delta P$  - Pressure drop
- $h$  - Heat transfer coefficient

$D_h$  - Hydraulic Diameter

$N_u$  - Nusselt number

### Acknowledgements

The authors acknowledge the encouragement & support rendered by the Microwave tube research & development center while carrying out this work

### References

- D.B. Tuckerman, R.F.W. Pease, (1981), High performance heatsinking for VLSI, *IEEE electron devices letter*, Vol. EDL-2, No 5
- K. Kawano, M. Sekimura, K. Minakami, H. Iwasaki, and M. Ishizuka, (2001), Development of micro channel heat exchanging, *JSME Int. J., Ser. B*, vol. 44, no. 4, 592–598.
- M. J. Kohl, S. I. Abdel-Khalik, S. M. Jeter, and D. L. Sadowski, (2005), An experimental investigation of microchannel flow with internal pressure measurements, *Int. J. Heat Mass Transf.*, vol. 48, no. 8, 1518–1533.
- R. Chein and J. Chuang, (2007), Experimental micro channel heat sink performance studies using nanofluids, *Int. J. Therm. Sci.*, vol. 46, no. 1, pp. 57–66.
- Fanghua Mei, Pritish R. Parida, Jing Jiang, Wen Jin Meng, and Srinath V. Ekkad, (2008), Fabrication, Assembly, and Testing of Cu- and Al-Based Micro channel Heat Exchangers, *Journal of Microelectro Mechanical Systems*, Vol., 17, No. 4
- Sean Ashman, Satish G. Kandlikar, (2006), A Review of manufacturing processes for micro channel heat exchanger fabrication, *Proceedings of ICNMM2006 Fourth International Conference on Nanochannels, Microchannels and Minichannels*, June 19-21, Limrick, Ireland
- Benjamin A. Jaspersen, Yonho Jeon, Kevin T. Turner, Frank E. Pfefferkorn, and Weilin Qu, (2010), Comparison of Micro-Pin-Fin and Micro channel Heat sinks considering Thermal-Hydraulic Performance and Manufacturability, *IEEE Transaction on components and packing technology*, Vol. 33, No. 1
- A. J. Pang, M.P.Y. Desmulliez, et al., (2004), Design, Manufacture and Testing of a Low-cost Micro-channel Cooling Device, *IEEE Conference on Electronics Packaging Technology*
- Choodal B. Soban and Suresh V. Garimells, (2001), A comparative analysis of studies on heat transfer and fluid flow in micro channels, *Microscale Thermophysical Engineering*, vol. 5, 291-311
- Weilin Qu, Issam Mudawar, (2002), Experimental and numerical study of pressure drop and heat transfer in a single-phase micro-channel heat sink, *International journal of Heat Mass Transfer*, vol. 45, pp. 2549-2565
- Ljubisa D. Stevanovic, Richard A. Beaupre, Arun V. Gowda, Adam G. Pautsch and Stephen A. Solocitz, (2010) Integral Micro-channel Liquid Cooling for Power Electronics, *Twenty-Fifth Annual IEEE, Applied Power Electronics Conference and Exposition (APEC), Palm springs, CA*, 21-25 Feb, pp. 1591-159.
- S. Subramanian, K.S. Sridhar, C.K. Umesh, (2014) Experimental & numerical study of forced convection laminar flow through copper micro channel heat sink, *International journal of Research in Engineering and Technology*, Vol. 03, no 12
- Y.J. Lee, P.S. Lee, S.K. Chou, (2013), Numerical study of fluid flow and heat transfer in the enhanced micro channel with oblique fins, *Journal of heat transfer*, vol. 135, pp. 04901-10.
- Laxmidhar Biswal, Suman Charborthy, and S.K. Som, (2009), Design and Optimization of Single-Phase Cooled Microchannel Heat Sink, *IEEE Transactions on Components and Packaging Technologies*, Vol. 32, no. 4, pp. 876-886.